Joint cost of energy under an optimal economic policy of hybrid power systems subject to uncertainty ☆

Guzmán Díaz[a,*], Estefanía Planas[b], Jon Andreu[c], Iñigo Kortabarria[c]

[a]Dep. of Electrical Engineering, University of Oviedo, Campus de Viesques, s/n, 33204 Spain
[b]Dep. of Electrical Engineering, University of the Basque Country UPV/EHU, Alameda Urkijo, s/n, 48013 Spain
[c]Dep. of Electronic Technology, University of the Basque Country UPV/EHU, Alameda Urkijo, s/n, 48013 Spain

Abstract

Economical optimization of hybrid systems is usually performed by means of LCoE calculation. Previous works deal with the LCoE calculation of the whole hybrid system disregarding an important issue: the stochastic component of the system units must be jointly considered. This paper deals with this issue and proposes a new fast optimal policy that properly calculates the LCoE of an hybrid system and finds the lowest LCoE. This proposed policy also considers the implied competition among power sources when variability of gas and electricity prices are taken into account. Additionally, it presents a comparative between the LCoE of the hybrid system and its individual technologies of generation by means of a fast and robust algorithm based on vector logical computation. Numerical case analyses based on realistic data are presented that valuate the contribution of technologies in an hybrid power system to the joint LCoE.

Keywords: Hybrid systems, optimization, LCoE

1. Introduction

The energy production based on renewable resources has been continuously increasing over the last decades due to the several advantages it reports. As the presence of distributed generation has increased, its integration into the main grid has become a critical point in order to preserve and guarantee the stability and quality of the mains grid. In this sense, electrical hybrid systems are a good option for connecting renewable energy production into the mains grid in a reliable and profitable manner.

As a definition, hybrid systems integrate different types of distributed generators in order to feed a local load [1]. These systems usually comprehend both renewable and non renewable energy sources and can incorporate storage systems. Among the research lines of hybrid systems, this paper deals with the optimization of the energy production from an economic point of view. Many works deal with the economic

☆This work has been carried out inside the Research and Education Unit UFI11/16 of the UPV/EHU and supported by the Department of Education, Universities and Research of the Basque Government within the fund for research groups of the Basque university system through: IT394-10, IE14-389 and DPI2014-53685-C2-2-R.

*Corresponding author
Email addresses: guzman@uniovi.es (Guzmán Díaz), estefania.planas@ehu.eus (Estefanía Planas), jon.andreu@ehu.eus (Jon Andreu), inigo.kortabarria@ehu.eus (Iñigo Kortabarria)

optimization of both standalone and grid connected hybrid systems. Regarding to stand-alone systems, in [2] cloud cover modeling is addressed in a standalone PV-battery system using Markov transition matrix of the clearness index. Another proposal can be found in [3] where an economic analysis of PV/diesel hybrid system with flywheel energy storage is performed. This economic analysis considers the power generation, energy cost, and net present cost. A stand-alone PV–wind–diesel system with batteries storage is also economically optimized in [4] by means of a multi-objective optimization that holds the levelized cost of energy (LCoE) and the equivalent carbon dioxide life cycle emissions (LCE) as objectives to be minimized.

According to grid connected hybrid systems, [5] recently proposed a planning technique using multi-objective optimisation formulation for a sustainable hybrid system including photovoltaic, wind turbine and battery energy storage systems. In this work, the objectives of the optimization function are the LCoE, embodied emissions of energy and the realiability generation. Apart from this, there is another proposal in [6] where a storage system is added to a private electricity facility with the aim of reducing the electricity bill. The work in [7] addresses the performance of a hybrid renewable system (consisting of a variable speed ICE and a solar device) for variable electricity prices by means of an optimised management strategy. Bortolini et al. proposed annother optimized hybrid system (photovoltaic system with battery energy storage) in [8]. This work deals with a model which optimizes the LCoE of an hybrid system and minimizes the LCoE of the system.

Taking into account the proposals found in the literature, economical optimizations of hybrid systems usually consider the Levelized Cost of Energy (LCoE). Although, the calculation of this LCoE is usually performed in a deterministic manner disregarding the uncertainty of the renewable sources. In [5] this uncertainty is modelled by means of method of moments. However, this method can be only applied with variables with a normal distribution. In addition, the LCoE of the whole hybrid system is normally calculated as the sum of the LCoE of the individual technologies, which is not a suitable method when uncertainty is involved. This paper aims to deal with these deficiencies and find an optimal policy for an hybrid power system under uncertainty.

The featured microgrid (MG) in this paper has three main generation technologies—small wind turbine, gas microturbine, and the main grid proper—entailing different conceptual approaches [9]. First, wind energy is a representative of a renewable-based energy source with a global installed capacity of almost 400 GW at the end of 2014 [10]. Its main characteristic is the uncertain, and somehow uncontrollable, power production level. Alternatively, thermal-based generation offers a remarkably higher certainty in power, but at the cost of more greenhouse gas emissions and increased operating costs. Both technologies are thus complementary, and in a MG they directly or indirectly affect the operation expenditures (OPEX). On the one hand, firing the thermal generation requires fuel consumption, with OPEX subject to the evolution of the gas price. Alternatively, renewable-based energy has almost negligible OPEX, but the uncertain power produced may make necessary buying power from the main grid. Though indirectly, this obviously has an impact on the MG OPEX. Supporting both technologies to increase reliability, the mains grid contributes to the OPEX also in a stochastic way.

This paper proposes a computation of the LCoE based on the premise that the MG has two major OPEX sources: gas and electricity purchases. Because gas and electricity prices do not necessarily follow correlated paths, the LCoE will vary depending on the energy mix; which ultimately will be driven by the mismatch between wind generation and load demand. This paper shows a computation of the LCoE based on an optimal policy, under which the OPEX is sought to be minimum by adequately switching between gas and electricity as a response to the power deficit originated by the load-generation mistmatch. The energy mix, and hence the OPEX, is sought to be optimal.

The main contributions of this paper are:

i. Foremost it demonstrates that the cost of energy in an hybrid system subject to different kinds of uncertainty cannot be simply extrapolated from the sum of costs of individual technologies.

ii. This is but a consequence of fact that stochastic variables cannot be directly summed. (At most if they were independent, they may be convoluted, but not directly summed [11].) To solve the problem, this paper features Monte Carlo experiments ensuing from a decomposition of the problem model into several; encompassing the uncertainties in the prices, loads, and wind power in auto-regressive models while retaining seasonal components.

iii. Compounding the problem, the existence of several technologies competing in costs makes it relevant to formulate an optimal policy to ensure that the cost of exploiting the hybrid system is minimal. But the classic approaches to optimization fail to be useful in this case because of the high dimensionality of an hourly scale problem over a year, repeated over a large number of Monte Carlo samples. This paper shows an alternative approach to find the optimal policy on the basis of vector logical operations, which gives both speed and simplicity at the time of determining the optimal scheduling of generating units.

iv. Finally, this paper confronts several scenarios from realistic data to analyze the contribution of hybrid systems to the LCoE formation; particularly comparing them with the sole import of electricity from the grid.

The paper is structured as follows. After an introduction explaining the main scopes and highlights of the work, a deep description of the hybrid system model is presented. In this description, LCoE concept is detailed and the implemented models are described: electricity price model, microturbine and gas price models, characterization of the load and wind power model. Later, the proposed optimal policy is presented which is discussed by means of a number of case analysis. Finally, the conclusions that are drawn from the article are presented.

2. Model characterization

2.1. Levelized cost of energy

The levelized cost of energy is the energy cost—in real euros—of building and operating a power-generating plant over its assumed financial life. In individual generating plants the components of the LCoE are readily interpreted. The building costs (hereafter CAPEX, for CApital EXpenses) consist of the expenditures incurred in the building of the plant. This paper considers that the CAPEX is expended only once, though in practice—depending on the technology lead time—it could be spread over a number of years.[1] Differently the term OPEX (for OPerating Expenses) covers the costs incurred in operating the plant every year over its lifetime. In this paper without loss of generality the OPEX is reduced to the fuel expenses.

The definition of LCoE has a built-in flexibility that allows for different interpretations and levels of detail; see for instance [12] and references therein. In this paper the definition employed is

$$LCOE = \frac{I_0 + \sum_{t=1}^{T} C_t \mathrm{e}^{-rt}}{\sum_{t=1}^{T} E_t \mathrm{e}^{-rt}}, \tag{1}$$

where

T is the financial lifetime of power-generating asset;

I_0 is the initial (capital) expenditures, the CAPEX;

C_t are the annualized costs of operation at year t, the OPEX;

E_t is the energy produced at year t; and

e^{-rt} is the *discount factor* at an interest rate equal to r, which discounts the yearly cash flows back to the present.

This formulation is readily applied to single generation units. Specifically, if the yearly produced energy is assumed to be constant over the entire lifetime (that is, $E_t = E$ for $t = 1, \ldots, T$), then

$$\sum_{t=1}^{T} E_t \mathrm{e}^{-rt} = \left[\frac{r(1+r)^T}{(1+r)^T - 1} \right] ET; \tag{2}$$

where the term within square brackets is termed the *capital recovery factor*. This simplification allows computing the LCoE once the capacity factor (CF) of the plant—the ratio of the yearly mean produced power to its maximum capacity—is estimated and the costs are known. However, this methodology is not adequate for evaluating the LCoE of an hybrid generation system subject to production uncertainty.

[1] *Overnight* costs is a way of reformulating I_0 when the expenditures are distributed over several years. It is a term employed in energy generation literature that essentially discounts back the distributed CAPEX to obtain one only equivalent expenditure. In practice, therefore, considering the cost accumulated in the first year does not represent a problem.

The generation paradigm approached in this paper is an hybrid grid-connected system as a means of supplying power to an aggregated load. From this viewpoint, the paper considers three types of generators, which encompass different definitions of OPEX, CAPEX, and produced energy. Wind turbines (WTs) represent a technology that has negligible OPEX (but for the O&M costs) because of the absence of input fuel. CAPEX are not negligible nonetheless. And importantly the power produced is subject to the uncertainty of wind availability. By contrast, microturbine (MT) production does not depend on the availability of the primary energy source. This paper considers full availability of gas. The uncertainty in this case occurs (indirectly) on the OPEX, which is subject to the gas market volatility. Finally, with some abstraction this paper considers the grid connection as a third generation technology. It is assumed that the power available from the grid is not subject to uncertainty. As with MTs, the uncertainty is not in the energy availability, but in the price; thus affecting the OPEX. Additionally, it is assumed that the CAPEX is zero for the grid connection, if we further assume that the connection must not be built.

From the above assumptions on uncertainty in the OPEX and power production, the computation of the LCoE for this type of systems cannot be directly specified by means of (1). The underlying OPEX components are stochastic in nature, but are not necessarily normally distributed; and therefore their aggregation to obtain the total OPEX cannot be obtained through direct arithmetic summation. Convolution can be applied in instances in which the variables are not normal but are independent, at the cost of calibrating the distributions and proceeding with the solution of multiple integrals. Alternatively, however, the underlying OPEX components can be characterized as stochastic processes, and the aggregation can be conducted as a sample approximation through a Monte Carlo experiment. Their characterization is the subject of what follows.

2.2. *Electricity price model*

One of the most commonly used methods for specifying the dynamics of the spot prices is the Ornstein-Uhlenbeck (OU) process. Formally, a generic OU process X_t satisfies the stochastic differential equation:

$$\mathrm{d}X_t = \lambda(\mu - X_t)\ \mathrm{d}t + \sigma\ \mathrm{d}W_t, \tag{3}$$

where $\mathrm{d}W_t = \varepsilon\sqrt{\mathrm{d}t}$, with $\varepsilon \sim N(0,1)$, are increments of the Wiener process.

The OU process is a mean-reverting process. It is a modification of the Wiener process—which is Markov, with independent increments, normally distributed, and with variance incrementing with the time interval—that forces the value of the process to revert to a long-run mean level. The reversion speed is λ, and μ is the mean level.

In [13] Lucia and Schwartz proposed a one factor model to characterize the spot price. Precisely the model followed an OU process with a relevant modification. They stated that the spot price P_t may be split into deterministic and stochastic components. Namely:

$$P_t = f(t) + X_t, \tag{4}$$

where the stochastic component X_t follows an OU model with zero long-run mean—that is, $\mu = 0$ in (3). Introducing $X_t = P_t - f(t)$ in (3), Lucia and Schwartz concluded that the spot price can be put in the form of a Hull-White process—an extension of the OU process—as follows:

$$\mathrm{d}P_t = \lambda(a(t) - P_t)\,\mathrm{d}t + \sigma\,\mathrm{d}W_t. \tag{5}$$

This model has an explicit solution,

$$P_t = f(t) + (P_{t-1} - f(t-1))\mathrm{e}^{-\lambda\Delta t} + \int_0^t \mathrm{e}^{\lambda(\tau-\Delta t)}\sigma\,\mathrm{d}W_t(\tau), \tag{6}$$

which entails that the price reverts to the mean value $f(t)$ in the long-run, subject to stochastic shocks. In the framework of this paper this is especially valuable, because it is the correlation between loads and prices—strongly affected by the seasonal, deterministic component—which determines the optimal policy leading to the lowest LCoE.

The extraction of the deterministic component requires some particular judgments about the electricity spot markets—what Geman and Roncoroni call *structural elements* in [14]. Hourly electricity prices are specifically subject to seasonal patterns at different scales. The most relevant is the intra-day seasonality, with differences between the weekdays and workdays. (In addition to this well-known intra-day patterns, other seasonalities have been reported in the literature; see for instance [15]. Nonetheless, to save space we have restricted our analysis to the intra-day seasonality, mindful that the addition of other seasonalities that depend on the price pressure in an individual market [14] is straightforward.)

We employed the hourly spot prices of the Spanish electricity market (OMIP) that covers the year 2014. To account for the seasonality, we regressed the spot price process on the time by employing a set of indicators. That is, we regressed

$$f(t) = \sum_{i=1}^{24} \beta_i \mathbf{1}_{\text{workday}}(t) + \sum_{i=25}^{48} \beta_i \mathbf{1}_{\text{Saturday}}(t) + \sum_{i=49}^{72} \beta_i \mathbf{1}_{\text{Sunday}}(t) \tag{7}$$

where $\mathbf{1}_A(x) := \begin{cases} 1 & \text{if } x \in A, \\ 0 & \text{if } x \notin A. \end{cases}$

To further facilitate the fitting of the spot price process of one year to the OU model we additionally removed the time-variant mean level. We employed a moving average filter of length 25 observations to compute it (filling the extremes of the ensuing series symmetrically with 12 constant values).

After removing the time-variant mean level—the deterministic component—we ended up with a stationary process. To check that it was stationary, we conducted Augmented Dickey–Fuller and Phillips-Perron tests to reject the null hypothesis of a unit root against an autoregressive alternative. These tests rejected the existence of a unit root with a 1% significance level. (In both cases the minimal p-value was 0.001.)

Table 1. Ornstein-Uhlenbeck process parameters.

Series	μ	σ	λ
Elec. price	-7.5×10^{-3}	321.38	1765.8
Gas price	-1.57	1.71	2.49
Hospital	-6.0934×10^{-4}	4.9784×10^{3}	2.9932×10^{3}
Large hotel	0.0164	2.4854×10^{3}	4.6366×10^{3}
Sec. School	-0.0015	4.2389×10^{3}	2.3074×10^{3}

Prices are given in €/MWh. Loads are given in W.

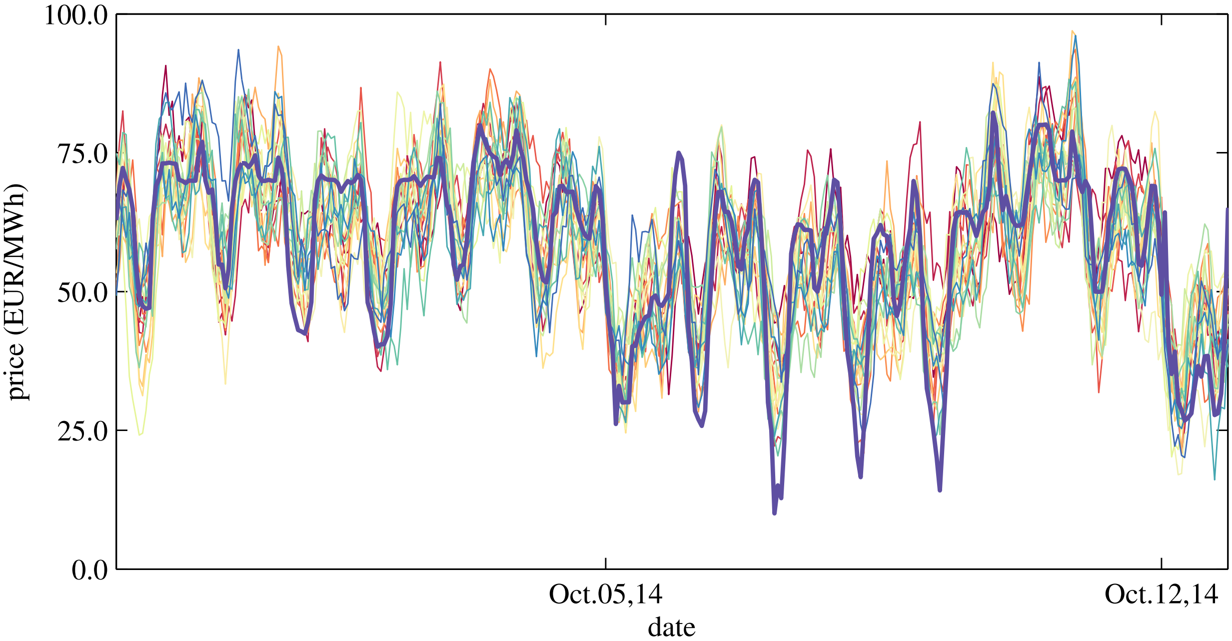

Fig. 1. Detail of a 15-sample simulation of hourly electricity price. The thick line is the original series.

The regression of the OU process to the stationary, stochastic component gave the values shown in Table 1 (Elec. price). As an illustration, a 15-sample simulation of the fitted OU process and the corresponding additive structural component is shown in Fig. 1.

2.3. *Gas-based generation*

2.3.1. *Microturbine model*

As an instance of fuel-based, non-intermittent power production, we selected MT generation. MTs are devices based on the conversion of the heating value of a fuel into electrical power and can be used to obtain Combined Heat and Power (CHP) [16, 17, 18]. Particularly, MTs are based on the Brayton cycle, which indicates that the power conversion is performed through four stages. A first stage compresses air to a value of typically four times the atmospheric pressure. Then, the exhaust air heats the compressed air just before it is mixed with gas. The gas ignites in the combustion chamber at a high temperature and expands through the turbine, leaving the exhaust the MT through the recuperator. In a single shaft MT a major part of the expansion work is directly delivered to the permanent magnet synchronous generator, rotating at some tens of thousands of rpm. A minor part of the expansion work is delivered to the compressor or lost as mechanical and hydraulic losses.

Modeling a MT is challenging since it comprises several layers of detail and can include both electric and thermal generation. In the core of the model is the ideal Brayton cycle, made up two isentropic and two isobaric processes. Refinements of the model include the inefficiency at this four processes and at the mechanic and electric energy conversion; with a degree of detail that depends on the model purpose. For the objective of this paper, it is evident that only the outer layer of these models is of real application—an outer layer that describes the gas mass flow rate employed to generate an unit of electrical power.

Badami and colleagues recently proposed in [19] a parsimonious model of a 100-kW gas MT. They modeled the electrical efficiency as

$$\eta_{\mathrm{MT}} = \frac{P_{\mathrm{MT}}}{\dot{V}_{\mathrm{g}} \times \mathrm{LHV}_{\mathrm{g}}}, \tag{8}$$

where P_{MT} is the electrical power, and $\dot{V}_{\mathrm{g}}$ and $\mathrm{LHV}_{\mathrm{g}}$ the volumetric flow rate and the low heating value of the gas. This efficiency directly provides the outer layer that will be required in the OPEX analysis. It is closely related to the specific fuel consumption (SFC), defined as the weight of fuel required to produce one kWh of electrical energy and employed to evaluate thermal generation (see for instance [20, Sec. 4 4], [21]), simply by stating that $\eta = \frac{1}{\mathrm{SFC} \times \mathrm{LHV}_{\mathrm{g}}}$.

Importantly Badami and colleagues demonstrated that the value of η_{MT} is not constant. According to their results, the SFC increases as the load reduces, which makes it less profitable to operate the MT at partial loads (see also [16]). We then elaborated their data to obtain a quadratic function representing the electrical efficiency. Thereafter, to obtain the cost of producing power by using the MT (i.e. the OPEX) we employed the Henry Hub natural gas spot price. The price, π_{g}, is given in dollars per million Btu. We employed the conversion 1 \$US/MBtu = 3.216 €/MWh. And because the conversion to €/kWh requires the LHV, eventually we defined the OPEX of the MT as:

$$C_{\mathrm{MT}} = \frac{\pi_{\mathrm{g}} \, P_{\mathrm{MT}} \, \Delta t}{-1.66 \times 10^{-2} P_{\mathrm{MT}}^2 + 4.18 \times 10^{-1} P_{\mathrm{MT}} + 6.56 \times 10^{-1}}. \tag{9}$$

2.3.2. *Gas price model*

To model π_{g} we followed a parallel approach to that for modeling the electricity price. Mean-reverting OU models have been also reported in the literature to adequately approximate the spot prices after extracting the deterministic components [22, 23]. However, the deterministic component at a low scale is not as easy observable in the gas as in the electricity prices. Gas prices are daily, and this makes it difficult to observe characteristic patterns as those shown in the electricity price. Therefore, we resorted in this case to differently extract the deterministic part by obtaining for each day the mean price over the last ten years [22]. The OU values obtained for gas price are shown in Table 1 (Gas price)

2.4. *Characterization of the load*

Many load forecasting methods can be found in literature as it is shown in the state of the art found in [24]. Loads are usually modelled by means of ARIMA models [25, 26, 27, 28] and normally consider puntual consumes (fridge, oven, TV, etc.). As these loads usually follow a seasonal pattern, we modelled these loads by means of parametric models in which the seasonal indicator is estimated. It is also interesting to notice that we considered the whole building (restaurant, hospital, house...) instead of an individual load (fridge, oven, TV...) as usual. Original load data has been exported from the OpenEI web site (`http://en.openei.org`). In table 1 (Hospital, Large hotel and Sec. School) and Fig. 2 the main parameters of the simulated loads are presented. The mean-reverting parameters in the table emphasize the different behavior of the stochastic component of the processes. For instance, the volatily of the hotel is half that of the shcool and the hospital. It serves to indicate that the deviations from the deterministic component are of lower amplitude in the hotel. The demand is less random. On the other hand, the speed of reversion, λ, assess the speed with which the deviations are suppressed. Again the hotel stochastic deviations are of shorter duration than those of the other two loads. (In this sense, by comparison of gas and electricity prices it is noticeable that electricity is more prone to large price spikes, as observed in its larger volatility. Also, the reversion is much faster. This is a feature that is readily observed in these two markets. A sudden unbalance of electric load is followed by a price spike, which is promptly restored by the System Operator, thus restoring the prices to the mean. However, gas prices are subject to arbitrage, what favors the deviation from the mean over longer periods.) In addition, these loads present different deterministic, seasonal patterns. For instance, secondary school presents a very similar pattern during the whole year: a similar consume from Monday to Friday and a minimal consume during weekend. This consume presents important changes during the summer weeks. The large office has a pattern for work days and another pattern for weekend days and a higher consume during central weeks of the year. In the case of the large hotel, a similar pattern is found for each day and a very stable demand is presented during the whole year. The hospital has a greater consume and a bigger difference of consume during the central weeks. It also presents different patterns for work days and weekend days.

2.5. *Wind power*

Wind power is the third source of power in this hybrid system, with uncertainty in the power production as its more relevant feature. In the previous characterization of stochastic processes—gas and electricity prices, and loads—we assumed that there was no autoregression beyond the mean reversion. For wind speed, however, our results showed that specifying the wind speed through this model did not prove to be accurate. However, in [29] the authors claimed to have investigated 54 wind datasets employing higher order autoregressive models in the form of ARMA(p, q). They concluded that the most frequent models were those described by $p = 1$ and $q \in [2, 4]$. In our case, following their lead we approximated data sets

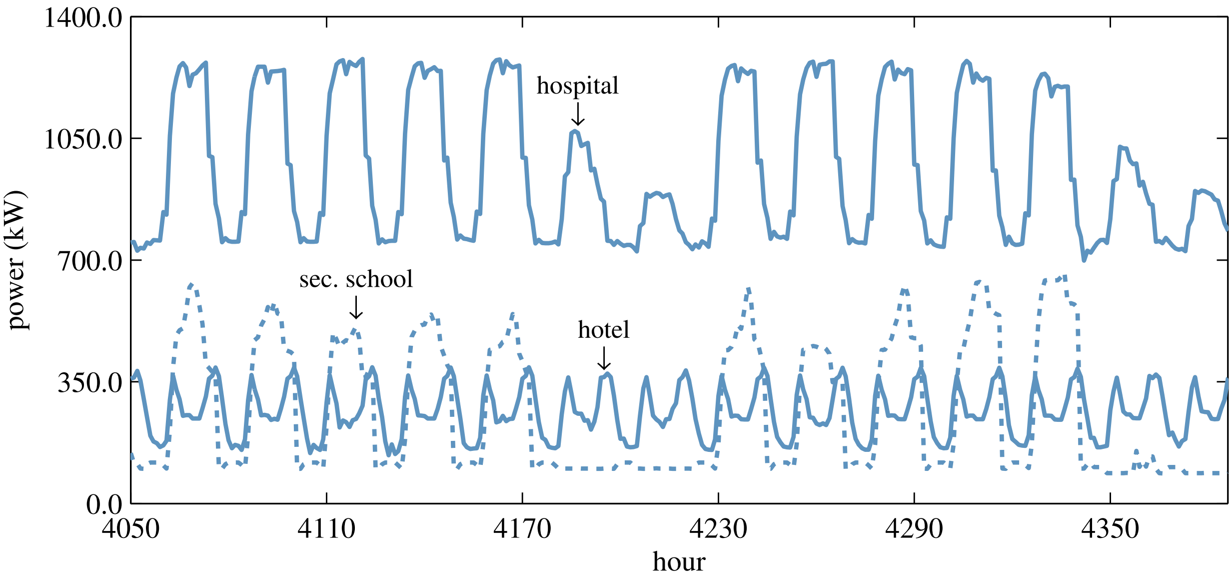

Fig. 2. Hourly load profiles for 2 weeks.

frrm `http://wind.nrel.gov/` by ARMA(1,3), with reasonable good accuracy. Particularly, we employed two different wind speed profiles, which we approximated through

$$w_t = 0.893w_{t-1} + \epsilon_t + 0.367\epsilon_{t-1} - 0.052\epsilon_{t-2} + 0.015\epsilon_{t-3},$$

which we call site 1, and

$$w_t = 0.917w_{t-1} + \epsilon_t + 0.294\epsilon_{t-1} - 0.025\epsilon_{t-2} + 0.001\epsilon_{t-3},$$

which we call site 2. The differences are depicted in Fig. 3 top.

The samples of wind speed must be subsequently transformed into wind power following the piecewise, nonlinear transformation characteristic of the turbine. Because the main subject of this paper was to investigate the LCoE of small hybrid systems, we resorted to model two small wind turbines—stall regulated—with relatively large differences. The Norwin 153 and the Bergley 53 differ not only in their maximum output power, but also in their characteristic wind speeds, as shown in Fig. 3. The Bergey starts producing at relatively lower cut-in wind speeds, but stops producing at visibly lower cut-off speeds. By comparison it is seen that the Bergey is nonetheless a good choice for site 1, where high wind speeds are not reached. In any case, as it is discussed below, it is this wide combination of wind speed distribution and WT characteristics what affects the LCoE.

3. Optimal policy

In this paper an optimal policy for power production is considered. This means that the generation scheduling is based on several levels of priority aimed at reducing the cost of generation; in this paper

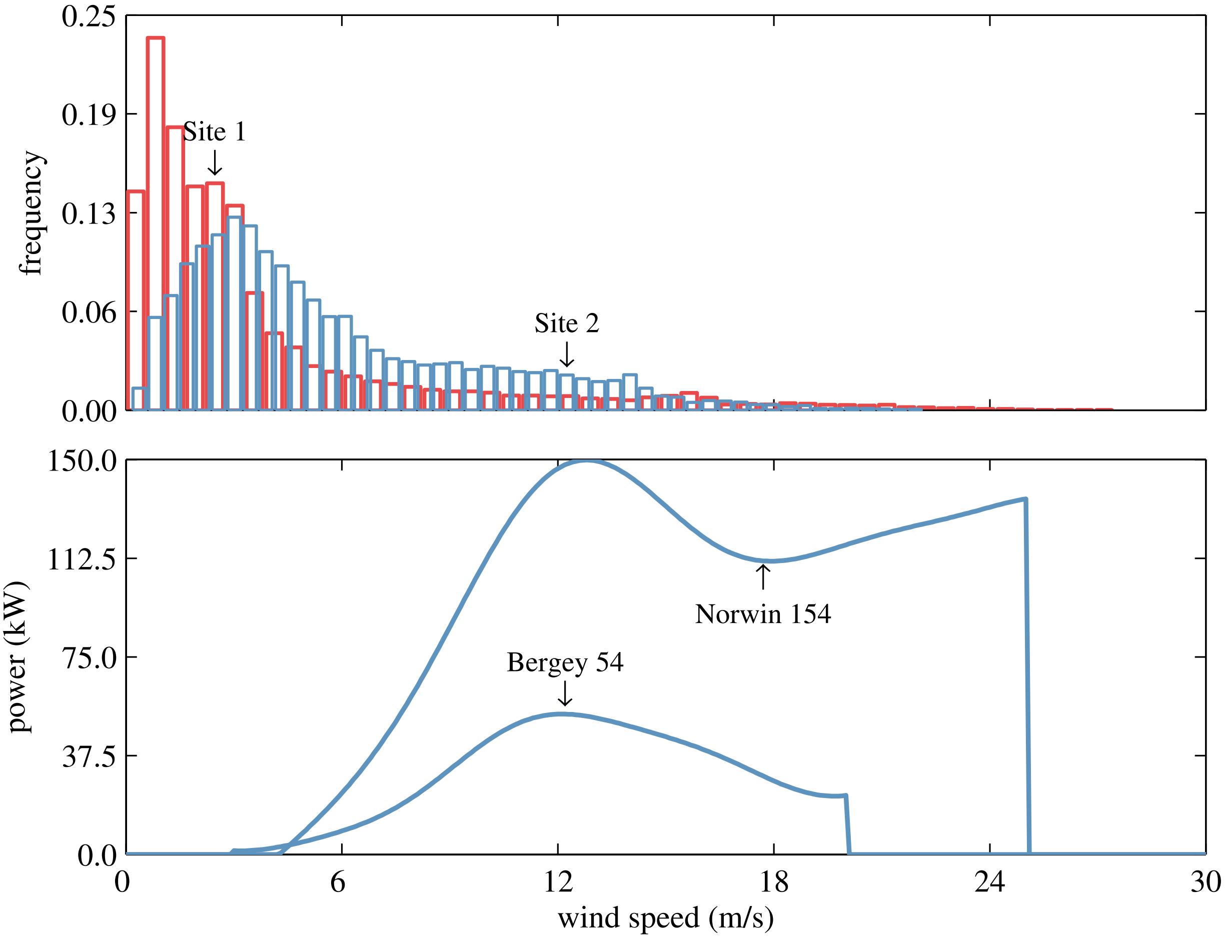

Fig. 3. Top: normalized frequencies of wind speed at sites 1 and 2. Bottom: wind power characteristics of the analyzed WTs.

the LCoE. The stratification of the priority is easy to perceive on the basis of the OPEX—the lowest OPEX should access the production first, being followed in OPEX ascending order by the rest of technologies. In the hybrid system presented in this paper only two technologies present non-null OPEX, namely the grid imports and the MT generation. Therefore, the problem may be stated as

$$\min_{P_{\mathrm{MT}}(t),P_{\mathrm{G}}(t)} \quad \sum_{t=1}^{T} \left[C_{\mathrm{MT}}(P_{\mathrm{MT}}, \pi_{\mathrm{g}}(t)) + \pi_{\mathrm{e}}(t) P_{\mathrm{G}}(t)\right] \tag{10a}$$

$$\text{s.t.} \quad P_{\mathrm{MT}}(t) + P_{\mathrm{G}}(t) + P_{\mathrm{WT}} = P_{\mathrm{L}}(t), \quad \forall t \tag{10b}$$

$$P_{\mathrm{MT}}^{\min} \leq P_{\mathrm{MT}}(t) \leq P_{\mathrm{MT}}^{\max}, \quad \forall t \tag{10c}$$

where C_{MT} is the MT OPEX, π_{e} the electricity price, P_{G} the electricity import, P_{WT} the wind power production, P_{L} is the load demand, $P_{\mathrm{MT}}^{\max}$ is the MT rated power (100 kW), and $P_{\mathrm{MT}}^{\min}$ is the technical minimum power of the MT (which we chose to be 50 kW).

As it is readily observed, this is but the optimal dispatch problem conventionally formulated in large power systems. However, the problem has the particularity of being of high dimension. By applying the capital recovery factor, we have reduced the problem from that covering the project whole lifetime (say 20 years) to a yearly problem. Still this problem presents a high dimensionality, because it is split into an hourly scale. Therefore, solving the problem by means of this conventional optimization approach under a Monte Carlo framework turns out to be too computationally expensive. (To put it into context, we employed 8760 periods over 10,000 Monte Carlo experiments. And each period includes two decision variables, namely the power generated by the MT and the power imported from the grid. The problem was tractable but would require several hours to solve for the 10,000-sample experiment.)

Because the problem incorporates only two decision variables at each period of a sample, we devised an alternative approach based on vector calculations which eventually gave the same results for every Monte Carlo experiment, but with compared negligible computational burden. It is clear that the two technologies competing for a slot in the hourly production are the grid energy import and the MTs. Unlike WTs, they usually exhibit non-zero CAPEX, which follow a stochastic evolution, as discussed before. Our procedure starts by assuming that the MT is always the technology of choice, and therefore it serves the load up to its maximum capability (100 kW) in every period:

$$P'_{\mathrm{MT}}(t) = \min\{P_{\mathrm{L}}(t) - P_{\mathrm{WT}}, P_{\mathrm{MT}}^{\max}\},\ t \in \mathcal{I} = 1, \ldots, T. \tag{11}$$

Subsequently, the MT is identified as the generation of choice only at those periods in which its OPEX is lower than that of the grid. So recalling that the MT OPEX is a function of P_{MT} as detailed in (9), then such periods of MT preference can be identified through the following index subset arising from a logical operation:

$$\mathcal{I}_{\mathrm{MT}} \subset \mathcal{I} = \left\{ t \in \mathcal{I} \,:\, \left[C_{\mathrm{MT}}(P'_{\mathrm{MT}}(t), \pi_{\mathrm{g}}(t)) \leq \pi_{\mathrm{e}}(t) P_{\mathrm{G}}(t) \right] \left[P_{\mathrm{L}}(t) - P_{\mathrm{WT}}(t) > P_{\mathrm{MT}}^{\min} \right] \right\}, \tag{12}$$

The optimal decision at period t is subsequently:

$$P_{\mathrm{G}}(t) = \begin{cases} \max\left\{0, P_{\mathrm{L}}(t) - P_{\mathrm{WT}}(t) - P'_{\mathrm{MT}}(t)\right\}, & \text{if } t \in \mathcal{I}_{\mathrm{MT}} \\ P_{\mathrm{L}}(t), & \text{otherwise} \end{cases} \tag{13}$$

$$P_{\mathrm{MT}}(t) = \begin{cases} P'_{\mathrm{MT}}(t), & \text{if } t \in \mathcal{I}_{\mathrm{MT}} \\ 0, & \text{otherwise} \end{cases} \tag{14}$$

The optimality is guaranteed because of the way in which the index set is built. The logical vector operation in (12) determines that the MT will be selected only when its operating cost, after subtracting the prioritary wind power, is less than the cost of importing electricity *and* at the same time it is within its generation bounds. This statement is equivalent to (10a) and (10c), because in the end the technologies of lower costs are given priority, which amounts to minimizing the total cost.

This structure is simple and robust, and it may be efficiently programmed in vector form,[2] speeding up the computation by several orders of magnitude when compared to the conventional optimization problem. It provides an optimal policy that selects the best technology at each period through (12) and accordingly assigns the load. The load is given to the less costly generation. When it is the MT and the load is in excess of its capability, the difference is assigned to the more costly grid.

In this optimal policy it can be easily corroborated that $P_{\mathrm{MT}}(t) + P_{\mathrm{G}}(t) + P_{\mathrm{WT}}(t) = P_{\mathrm{L}}(t), \forall t \in \mathcal{I}$, as required in (10). This results is inherent to the way in which we proceeded by directly subtracting the available wind power to the load demand. This was indeed possible because of the null wind power CAPEX, that avoids taking the power production by the WTs as decision variables. (Indeed, it is but a particularization of the merit order observed in large power systems.) This clearly simplifies the problem, but moreover it evidences a side effect on the provision of technologies with null CAPEX. Specifically, it may occur that the net power $P_{\mathrm{L}}(t) - P_{\mathrm{WT}}(t)$ introduced in (11)–(14) is negative. In those cases, the excess wind power can be spilled or sold—when so regulated—at a given price. We have considered both scenarios to investigate how this possibility of selling the excess power affect the LCoE. But importantly, the only modification required to contemplate these scenarios is to supply an additional constraint to (11)–(14), namely

$$P_{\mathrm{WT}}(t) = \min\{P_{\mathrm{WT}}(t), P_{\mathrm{L}}(t)\}, \tag{15}$$

when the excess wind power is spilled. This retains the simplicity and robustness of the algorithm.

The ensuing optimal policy obtained through the previous model is summarized in the one-sample, one-week plot of Fig. 4. The scheduling of power production is made on the basis of the comparison of the OPEX of grid energy import and MT production. The former is straightforwardly related to the electricity price, π_{e}, and therefore the different daily and hourly patterns arising from the modeling procedure explained in Section 2.2 are evident. The MT OPEX is obtained through (9), and therefore it is a modified version of the daily gas price, π_{g}. Equally, the patterns of daily and hourly load demand (of a secondary school in this example) are retained in the simulation, as observed in the bottom plot, where the weekdays and weekend are clearly observed.

Details of the proposed optimal policy are clearly observed in the bottom panel. For instance during the first fourteen hours, the MT CAPEX is lower than that of the grid, this entailing that the MT will produce at rated power (100 kW), while the rest of the load is complemented by energy import at a more higher cost. The 100-kW limitation is clearly observed as a plateau, with some small indentations over the first hours, when the load is a bit less than 100 kW and the turbine reduces its output. Over the next 24 hours the simulated wind speed is within the cut-in and cut-off speeds of the WT, and therefore its power is first delivered (because of its null CAPEX), with the MT following next to complete the load (because its

[2] See Octave/Matlab for instance.

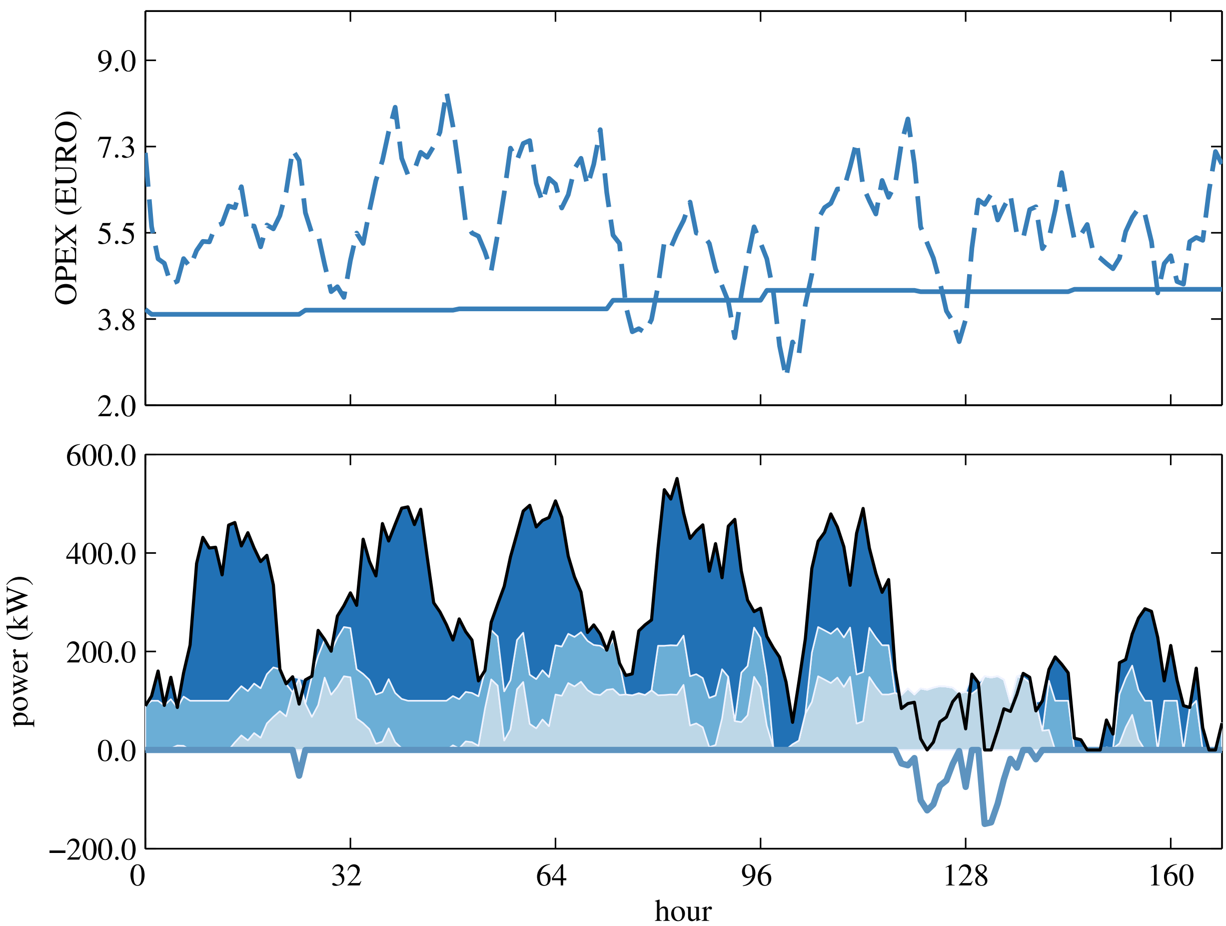

Fig. 4. Optimal policy illustration. Top panel: computed OPEX of grid energy import (dashed line) and of MT (solid line) for a constant 100-kW power generation. Bottom panel: power dispatch to satisfy the load demand of the secondary school (black line) by means of wind power (light shade), MT power (medium shade), and grid energy import (darkest shade). The blue line below zero represents excess power production.

CAPEX is still lower than that of the grid), and finally the expensive grid accounting for the rest of the load. It can be observed that the reduction of the load demand at hour 24 provokes a surplus production, which is detailed as the negative peak in the plot. This is again repeated more clearly at around hour 128 (weekend). When this occurs, the problem bifurcates depending on whether the excess power is spilled or can be recovered by selling it to the grid. Also it is noted how when the OPEX of the grid in the top panel falls below that of the MT, the power dispatch changes in the bottom panel because of the shut down of the MT. Still, it can be observed that the wind power delivery retains its priority in either case.

4. Case analysis

In what follows we discuss the results from diverse scenarios through the observation of the classic Tukey box plots ensuing from the simulations. The sample size was $K = 1000$ with $N = 8760$ observations.

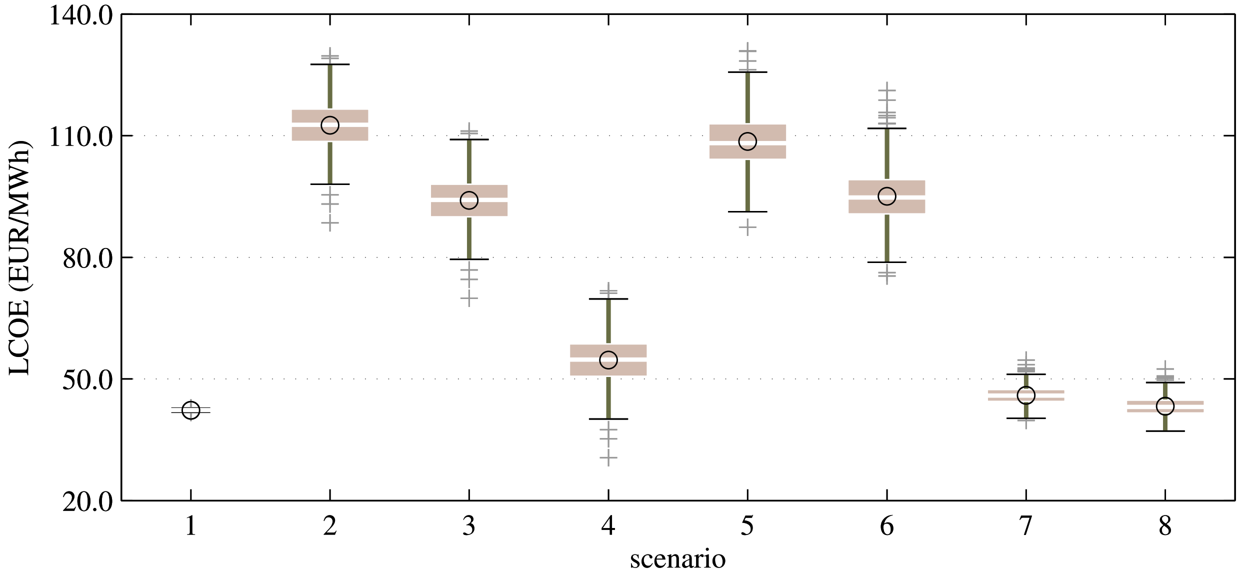

Fig. 5. Tukey's box plots comparing the distributions of CLoE of single units, performing at their maximum capacity. Scenario 1: equivalent cost of importing electricity from the grid. Scenarios 2 through 4: only a MT with decreasing CAPEX. Scenarios 5 and 6: different WTs at a low resource wind site. Senarios 7 and 8: as in 5 and 6, but with better wind speed profile.

Table 2. Scenarios of Fig. 5.

Scenario	Element
1	Grid
2	MT with a CAPEX of 33 k€
3	MT with a CAPEX of 20 k€
4	MT with a CAPEX of 0 k€
5	WT Bergey 53 in wind site 1
6	WT Norwin 153 in wind site 1
7	WT Bergey 53 in wind site 2
8	WT Norwin 153 in wind site 2

4.1. Analysis of LCoE for individual technologies

First, generation costs of individual technologies are compared with the equivalent cost of bulk generation supplied by the grid (Fig. 5 and Table 2). The grid CAPEX is considered null in this analysis, and the ensuing LCoE—indeed the cost of power purchase to the grid—is shown in the first scenario of Fig. 5. The mean LCoE is 42.3 €; with very low uncertainty if the interquartile range (IQR) equal to 0.2 €/MWh is taken as a measure of uncertainty. Note that the low IQR does not mean that the prices did not fluctuate more than that value. (Indeed our simulated data ranged from 0 through 109.6 €/MWh for the electricity purchases, over the year 2014 and the 1000 samples.) What it means is that the sample variability in the whole LCoE over the 1000 samples was low, with first and third quartiles amounting to 42.2 and 42.4 €/MWh.

Such low central tendency and variability of the grid LCoE is not replicated when the 100-kW power

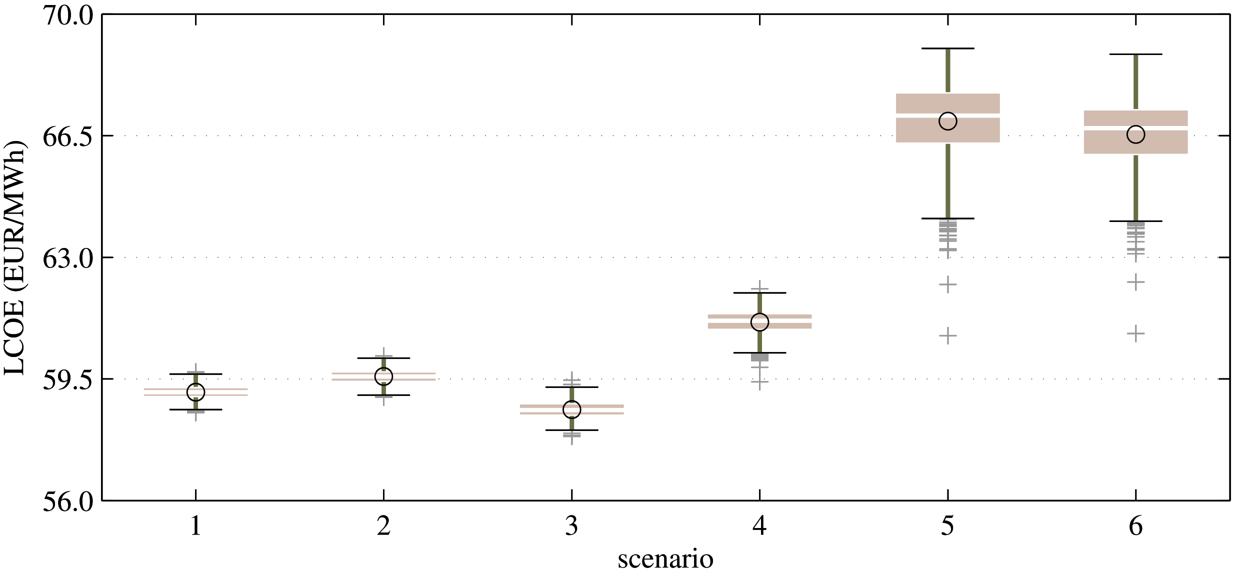

Fig. 6. Illustration of the increase in LCoE ensuing from the introduction of MT. Scenarios 1 through 3: only grid support for suppling load to thee hospital, hotel, and school, respectively. Scenarios 4 through 6: same as 1 through 3, but with additional support by a MT. See Table 3.

generation is provided by the gas MT. Scenarios 2 through 4 represent the MT generation system with decreasing CAPEX values. The sample variability of the LCoE is visibly higher than that of the sole grid; inherited from the higher accumulated deviation of yearly gas prices because of its lower reversion speed. Scenario 2 had an annualized CAPEX equal to 33.0 k€ (with a CRF equal to 9.4% ensuing from a 7.0% WACC and 20 years of assumed lifetime), and that of scenario 3 was 20.0 €. These were the annualized CAPEX computed from the range of CAPEX given by Lazard for MTs. Scenario 4 shows an alternative, hypothetical case in which the MT CAPEX was null. In any case, the results show that MTs are not competitive in supplying a constant 100-kWh load. Some few samples do get lower LCoE for MTs than for grid energy provision, but only when the CAPEX is artificially zero. (It must be emphasized that this analysis arises from considering null grid CAPEX. This is arguable and if the grid connection is taken into account, then obviously an upward displacement of the data of scenario 1 in Fig. 5 would occur; questioning the competitiveness of the MTs.)

Generation by means of WTs features a higher variability in the ensuing LCoE. Scenarios 5 and 6 depict the generation cost when Bergey 53 and Norwin 153 WT are employed in the wind site 1. The cost is comparable to that of the MT, with the Bergey MT featuring worse LCoE because of reduced working range. On the contrary, the LCoE is competitive when the wind site 2 is analyzed instead.

4.2. *Analysis of LCoE with grid importation and MT*

The previous analysis is straightforward, and the results may be inferred from conventional LCoE computation. The values agree with those published by Lazard. However, when several generation alternatives

Table 3. Scenarios of Fig. 6.

Scenario	Grid	MT	Load		
			Hospital	Large Hotel	Sec. School
1	✓		✓		
2	✓			✓	
3	✓				✓
4	✓	✓	✓		
5	✓	✓		✓	
6	✓	✓			✓

Table 4. CFs of Fig. 6.

Scenario	1	2	3	4	5	6
Grid	1.000	1.000	1.000	0.962	0.863	0.880
MT	0.000	0.000	0.000	0.341	0.340	0.288

are present—abiding optimal generation policies subject to variable loads—the computation and interpretation of the LCoE is more involved. Fig. 6 with Table 3 analyzes the LCoE ensuing from joint grid import and MT generation. The first three scenarios describe the power supply with only grid electricity import to a hospital, a large hotel, and a secondary school, respectively. The hospital is the largest load, demanding 7.9 MWh/year, with power ranging from 1.4 MW through 64.7 kW. The hotel demand (2.17 MWh, with power in the range 24.7 through 519.0 kW) is a repetitive load that has low weakly seasonality, but a marked daily seasonality. Finally, the school demand has a strong weekly seasonality, with demand almost null in weekends and loads topping 791.8 kW during weekdays. Remarkably, the amount of yearly consumed energy is quite similar in the hotel and school (2.17 and 2.10 MWh), but they are specifically differentiated by their seasonality and load level variability.

The differences in the LCoE of the grid-only paradigm supporting the three loads are not significant; around 58 €/MWh. We point out, however, that this is about 10 €/MWh more expensive than when a constant load is supplied. The reason is that now the more expensive day hours are not compensated with a same level of load over the cheaper night hours. The MT generation does not serve to cut down the cost of generation, however. Again the CAPEX is excessively high. But the differences in the LCoE are more remarkable nonetheless. The hospital supply (scenario 4) has the lowest LCoE, and the school LCoE is slightly lower than that of the hotel (though it may be argued that the difference is not representative).

Table 4 provides guidance on how to explain the differences. We define the CF of the MT over K samples as:

$$CF_{\mathrm{MT}} = \frac{\sum_{k=1}^{K}\sum_{t=1}^{N} E^{*}_{\mathrm{MT},k}(t)}{8760 \times K \times P^{\max}_{\mathrm{MT}}}, \tag{16}$$

where $E^{*}_{\mathrm{MT},k}(t)$ is the energy produced in the k-th sample at period t under an optimal policy, and $P^{\max}_{\mathrm{MT}}$ is the maximum power output of the MT. (Equally the CF of the WT can be defined, but replacing the corresponding terms of energy and power.) Because the grid is assumed to have no maximum power cap,

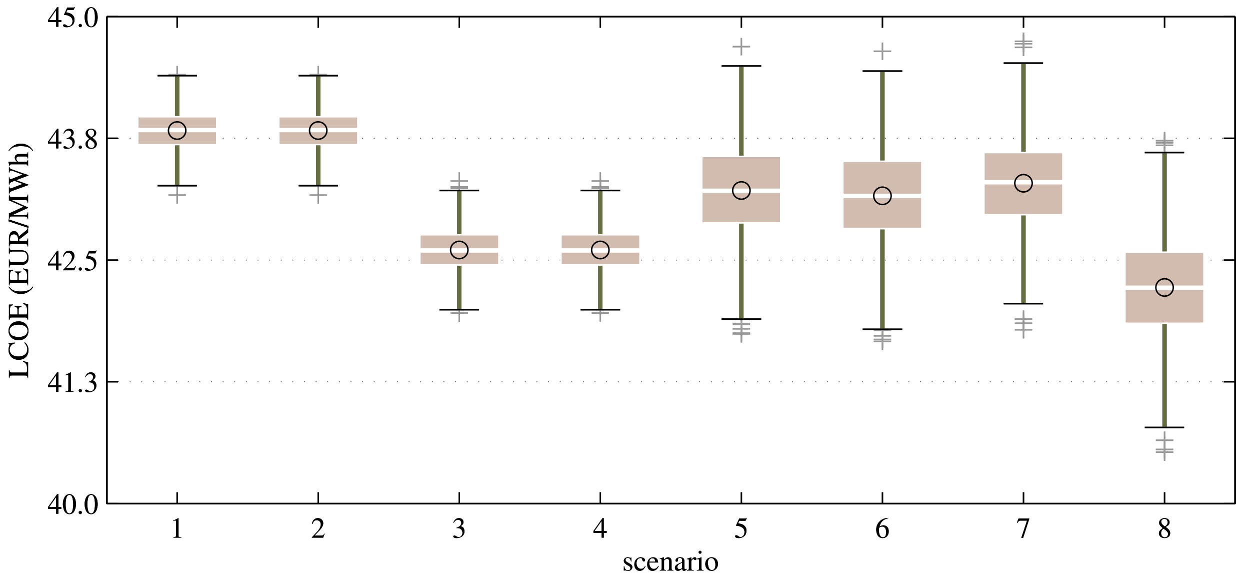

Fig. 7. Impact of wind and load power pairing. (No MTs are considered here.) Comparison of the differences in LCoE after curtailing (odd scenarios) or saling (even scenarios) the excess power when available. The two first scenarios depict low wind resources. Because the excess power depends on the correlation between loads and wind, different loads are employed, as detailed in Table 5.

we alternatively defined the CF of the grid as:

$$CF_{\mathrm{G}} = \frac{\sum_{k=1}^{K} \sum_{t=1}^{N} E^{*}_{\mathrm{G},k}(t)}{\sum_{k=1}^{K} \sum_{t=1}^{N} E_{\mathrm{L},k}(t)}, \tag{17}$$

where $E^{*}_{\mathrm{G},k}(t)$ is the energy imported from the grid under an optimal policy, and $E_{\mathrm{L},k}(t)$ is the energy demanded by the load.

First, 96.2% of the hospital (large) energy demand is supplied by the grid, with the MT at its optimal maximum capacity (34.1%, for the given gas and electricity price samples and the load profile). The contribution of the MT annualized CAPEX to increase the LCoE is hidden by the large grid OPEX. Contrarily, the optimal policy in the hotel and school reduces the contribution of the grid to around 87% because the excess of demand when the MT is entered is reduced. We see that the MT CF is close to its maximum (in 34.0% of the observations the MT generation was more profitable than importing electric power), indicating that it was necessary to still import electricity at times of electricity high prices. In the school, the MT does not achieve the economic maximum CF, showing that grid OPEX was more advantageous than that of gas; despite of the lack of demand in weekends when the electricity prices are expected to be lower.

4.3. Analysis of LCoE with grid importation and WTs

Fig. 7 shows the results of supplying the same loads as in Fig. 6 by grid and wind joint generation (Scenarios detailed in Table 5). All the analysis considered the Norwin 153 with minimum CAPEX as the WT of choice because of its higher production. As expected, the LCoE is significantly reduced compared

Table 5. Scenarios of Fig. 7.

Scenario	Grid	WT (Norwin 153) Side 1	Side 2	Load Hospital	Large Hotel	Sec. School	Excess wind energy Curt.	Sale
1	✓	✓		✓			✓	
2	✓	✓		✓				✓
3	✓		✓	✓			✓	
4	✓		✓	✓				✓
5	✓		✓		✓		✓	
6	✓		✓		✓			✓
7	✓		✓			✓	✓	
8	✓		✓			✓		✓

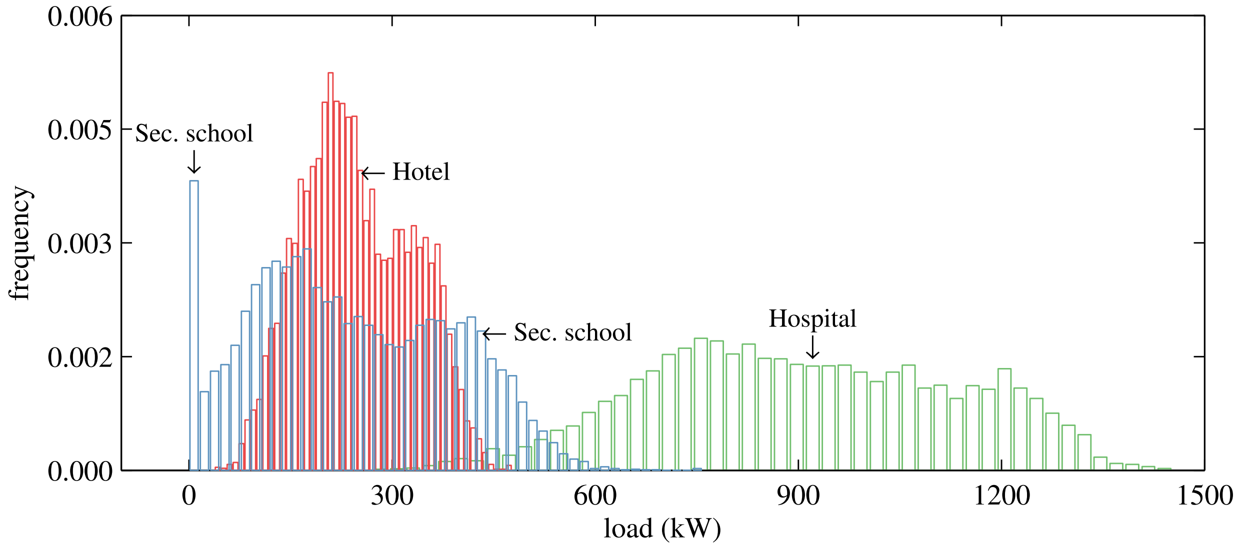

Fig. 8. Frequency of the load levels of the featured loads: hospital (green), large hotel (red), and secondary school (blue).

to Fig. 6, because of the null OPEX, and depending on the wind resource. Scenarios 1 and 2 (site 1) should be compared to 3 and 4 (more windy site 2) to assess the impact of the wind speed on the LCoE. In the four cases the load is the hospital and it is clear how the increment of the WT CF from 14.4% (1 and 2) to 31.6% (3 and 4) provides and improvement over the grid-only option—recall that the central tendency of the grid-only LCoE was 42.3 €/MWh. Yet this conclusion could not have been directly drawn from individual data.

Odd and even scenarios represent curtailment and sale of excess wind power, respectively. Scenarios 3 through 8 (all for wind site 2) correspond to the hospital, hotel, and school. As expected, the LCoE for the hospital is unaffected by the possibility of excess energy sale, because there is not a possibility of power spilling (the hospital load is too high). Alternatively, the hotel exhibits an almost imperceptible LCoE reduction when the excess energy sale is allowed (scenario 6, compared with curtailment in scenario 5). It is remarkable when compared with the hospital, however, how the distribution has longer tails in the case

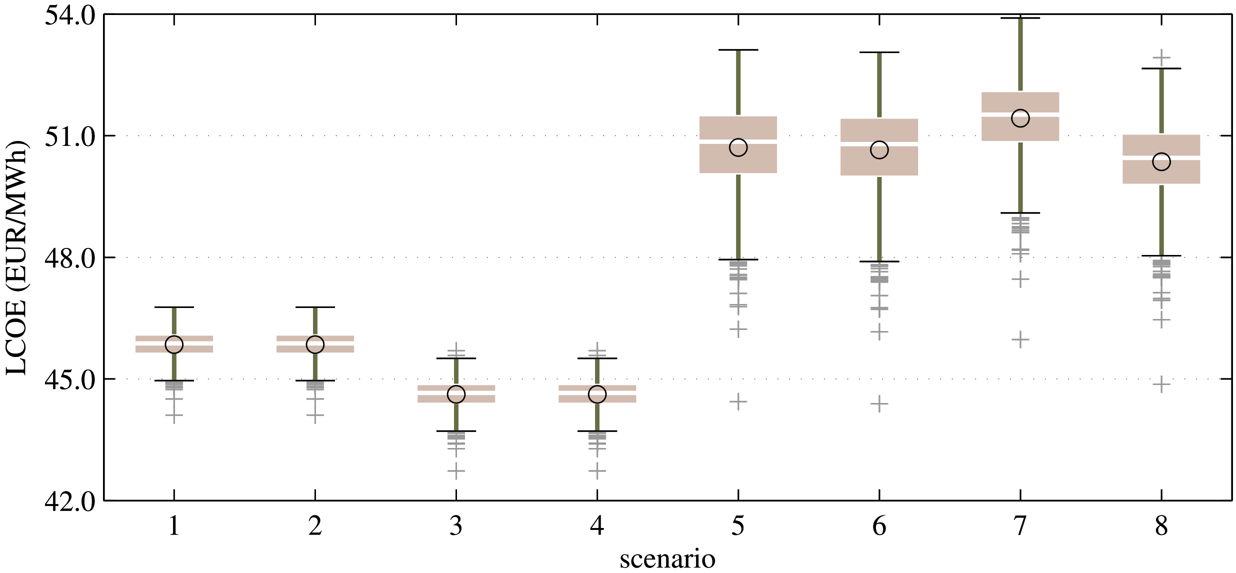

Fig. 9. Impact of all generation technologies. Same scenarios as in Fig. 7, but including also the MT.

of the hotel, reflecting the larger uncertainty in the LCoE introduced by the larger wind power share. But it is in the case of the school where the differences are more significant. Scenario 8, though again with high variability, displays the lowest LCoE—even considering that its energy demand and that of the hotel was almost equal. The reason for this LCoE reduction can be inferred from the CF analysis and the frequency plots of Fig. 8. It is clear that the minimum load of the hospital is far higher than the maximum WT output (153 kW), which entails no excess production with a CF of 31.6% in both scenarios 3 and 4. Contrarily in the case of the hotel, there are some chances of excess power. However, the computed Spearman correlation is as low as 0.019, which means that the options for spilling power are quite reduced—indeed the CFs with curtailment and with energy sale are 31.3% and 31.6%, respectively. In the secondary school is significant, however, the large zero counts in Fig. 8, probably arising from the frequent shutdown at weekends. This obviously improves the chances of existing excess energy. As a consequence, the "free" energy curtailed slightly increases the LCoE (scenario 7), and when the sale is allowed reduces it (scenario 8); though the traded energy is almost the same as in scenarios 5 and 6.

Again it must be remarked the difficult in finding this different LCoE values based only on individual accounts of LCoE of the different types of generation involved.

4.4. Analysis of LCoE with all generation technologies

Finally Fig. 9 repeats the analysis in Fig. 7, but in this case both MT and WT generation are considered. As in the previous analysis, recovering the otherwise curtailed power improves the LCoE. But the introduction of the MT worsens all the scenarios where only WT was before considered. Though the MT reduces the effective load power when it is fired—thus giving more chance to wind power recovery—the

Table 6. Scenarios of Fig. 9.

Scenario	Grid	WT (Norwin 153) Side 1	Side 2	MT	Load Hospital	Large Hotel	Sec. School	Excess wind energy Curt.	Sale
1	✓	✓		✓	✓			✓	
2	✓	✓		✓	✓				✓
3	✓		✓	✓	✓			✓	
4	✓		✓	✓	✓				✓
5	✓		✓	✓		✓		✓	
6	✓		✓	✓		✓			✓
7	✓		✓	✓			✓	✓	
8	✓		✓	✓			✓		✓

ensuing arbitrage is not enough profitable so as to curb the large CAPEX increase. The difference between scenarios 7 and 8 is larger, precisely because the recovered wind power is larger; were it allowed. But compared to scenarios 7 and 8 of Fig. 9, the LCoE is much higher, though not so high as when grid and MT are the two energy sources.

5. Conclusions

This paper contemplates two main problems in the formation of the LCoE of hybrid power systems in which renewable and thermal generation, along with conventional grid supply, are jointly employed. First, it is the stochastic nature of the variables involved that precludes the direct summation of LCoEs from individual power sources. The stochastic feature occurs because of the uncertainty on electricity and gas prices—affecting the operational costs—and on the power production of renewable sources. Secondly, the variability of gas and electricity prices provokes a competition between derived power sources.

In this paper we have proposed an stochastic Monte Carlo experiment that includes a fast optimal policy computation routine to tackle the two problems and obtain the combined LCoE. It precisely computes the LCoE with the deterministic and stochastic components of the elements involved, and it expands the analysis to large samples to provide an estimate of the LCoE under the existing uncertainties and valuate the contribution of different power sources to the joint LCoE.

The interrelationships in the LCoE formation when several technologies are jointly considered are highlighted. Importantly, it is evidenced in the results of this paper that the LCoE is not formed through easy computation from (published) records of separate technologies. For instance in our analysis, the central tendency of grid and MT LCoEs were 42.3 and 111.3 €/MWh for a unity capacity factor (CF) when considered individualy.. However, this paper shows that when they are jointly producing under an optimal policy, the LCoE is scenario dependent. Moreover, the LCoE depends on the load profile, which indeed can be assumed to be negative generation. The proposed valuation algorithm returns 61.7 €/MWh for a hospital load (after computing a 34.1% CF for the MT and 96.2% share of energy by the grid) and 67.1 €/MWh for a hotel load (when the returned CF is also 34.0% but the grid share is reduced). This shows that the computation of LCoE from published data about separate technologies does not allow a prompt calculation of the joint LCoE.

References

[1] A. H. Fathima, K. Palanisamy, Optimization in microgrids with hybrid energy systems – a review, Renewable and Sustainable Energy Reviews 45 (2015) 431 – 446.

[2] A. Bouabdallah, J. Olivier, S. Bourguet, M. Machmoum, E. Schaeffer, Safe sizing methodology applied to a standalone photovoltaic system, Renewable Energy 80 (2015) 266 – 274.

[3] M. A. Ramli, A. Hiendro, S. Twaha, Economic analysis of pv/diesel hybrid system with flywheel energy storage, Renewable Energy 78 (2015) 398 – 405.

[4] R. Dufo-López, J. L. Bernal-Agustín, J. M. Yusta-Loyo, J. A. Domínguez-Navarro, I. J. Ramírez-Rosado, J. Lujano, I. Aso, Multi-objective optimization minimizing cost and life cycle emissions of stand-alone pv–wind–diesel systems with batteries storage, Applied Energy 88 (2011) 4033 – 4041.

[5] M. Abdullah, K. Muttaqi, A. Agalgaonkar, Sustainable energy system design with distributed renewable resources considering economic, environmental and uncertainty aspects, Renewable Energy 78 (2015) 165 – 172.

[6] R. Dufo-López, Optimisation of size and control of grid-connected storage under real time electricity pricing conditions, Applied Energy 140 (2015) 395 – 408.

[7] C. Brandoni, M. Renzi, F. Caresana, F. Polonara, Simulation of hybrid renewable microgeneration systems for variable electricity prices, Applied Thermal Engineering 71 (2014) 667 – 676. Special Issue: {MICROGEN} III: Promoting the transition to high efficiency distributed energy systems.

[8] M. Bortolini, M. Gamberi, A. Graziani, Technical and economic design of photovoltaic and battery energy storage system, Energy Conversion and Management 86 (2014) 81 – 92.

[9] S. Mallikarjun, H. F. Lewis, Energy technology allocation for distributed energy resources: A strategic technology-policy framework, Energy 72 (2014) 783–799.

[10] G. W. E. Council, www.gwec.net (2015).

[11] G. Díaz, J. Gómez-Aleixandre, J. Coto, Statistical characterization of aggregated wind power from small clusters of generators, International Journal of Electrical Power & Energy Systems 62 (2014) 273–283.

[12] A. Levitt, W. Kempton, A. Smith, W. Musial, J. Firestone, Pricing offshore wind power, Energy Policy (2011).

[13] J. J. Lucia, E. S. Schwartz, Electricity Prices and Power Derivatives: Evidence from the Nordic Power Exchange, Review of Derivatives Research 5 (2002) 5–50.

[14] H. Geman, A. Roncoroni, Understanding the Fine Structure of Electricity Prices*, The Journal of Business (2006).

[15] C. R. Knittel, M. R. Roberts, An empirical examination of restructured electricity prices, Energy Economics 27 (2005) 791–817.

[16] J. Kaikko, J. Backman, Technical and economic performance analysis for a microturbine in combined heat and power generation, Energy 32 (2007) 378 – 387. {ECOS} 05. 18th International Conference on Efficiency, Cost, Optimization, Simulation, and Environmental Impact of Energy Systems {ECOS} 05.

[17] V. Kuhn, J. Klemeš, I. Bulatov, Microchp: Overview of selected technologies, products and field test results, Applied Thermal Engineering 28 (2008) 2039 – 2048. Selected Papers from the 10th Conference on Process Integration,Modelling and Optimisation for Energy Saving and Pollution Reduction.

[18] H. Cho, A. D. Smith, P. Mago, Combined cooling, heating and power: A review of performance improvement and optimization, Applied Energy 136 (2014) 168 – 185.

[19] M. Badami, M. G. Ferrero, A. Portoraro, Dynamic parsimonious model and experimental validation of a gas microturbine at part-load conditions, Applied Thermal Engineering 75 (2015) 14 – 23.

[20] N. Petchers, Combined heating, cooling & power handbook : technologies & applications. An integrated approach to energy resource optimization, The Fairmont Press, New York, NY, 2012.

[21] K. Sim, B. Koo, C. H. Kim, T. H. Kim, Development and performance measurement of micro-power pack using micro-gas turbine driven automotive alternators, Applied Energy 102 (2013) 309–319.

[22] H. van Goor, B. Scholtens, Modeling natural gas price volatility: The case of the UK gas market, Energy 72 (2014) 126–134.

[23] Y. Kitapbayev, J. Moriarty, P. Mancarella, Stochastic control and real options valuation of thermal storage-enabled demand response from flexible district energy systems, Applied Energy 137 (2015) 823–831.

[24] N. Sisworahardjo, A. El-Keib, J. Choi, J. Valenzuela, R. Brooks, I. El-Agtal, A stochastic load model for an electricity market, Electric Power Systems Research 76 (2006) 500 – 508.

[25] C.-M. Lee, C.-N. Ko, Short-term load forecasting using lifting scheme and {ARIMA} models, Expert Systems with Applications 38 (2011) 5902 – 5911.

[26] Y.-K. Seo, W.-H. Hong, Constructing electricity load profile and formulating load pattern for urban apartment in korea, Energy and Buildings 78 (2014) 222 – 230.

[27] M. Khashei, M. Bijari, A novel hybridization of artificial neural networks and {ARIMA} models for time series forecasting, Applied Soft Computing 11 (2011) 2664 – 2675. The Impact of Soft Computing for the Progress of Artificial Intelligence.

[28] Y. Wang, J. Wang, G. Zhao, Y. Dong, Application of residual modification approach in seasonal {ARIMA} for electricity demand forecasting: A case study of china, Energy Policy 48 (2012) 284 – 294.

[29] J. Torres, A. García, M. De Blas, A. De Francisco, Forecast of hourly average wind speed with ARMA models in Navarre (Spain), Solar Energy 79 (2005) 65–77.